

[Invited Paper]

## Nanotribological properties of silicon nano-pillars coated by a Z-DOL lubricating film<sup>†</sup>

Duc Cuong Pham<sup>1,2</sup>, Kyunghwan Na<sup>1</sup>, Sungwook Yang<sup>1</sup>, Jinseok Kim<sup>1</sup> and Eui-Sung Yoon<sup>1,\*</sup><sup>1</sup>Nanobio Research Center, Korea Institute of Science and Technology, Seoul 136-791, South Korea<sup>2</sup>Department of Mechanical Engineering, Hanoi University of Technology, No1 DaiCoViet, Hanoi, Vietnam

(Manuscript Received August 26, 2009; Revised September 11, 2009; Accepted October 12, 2009)

### Abstract

This paper reports a novel approach for improving the nanotribological properties of silicon (Si) surfaces by topographically and chemically modifying the surfaces. In the first step, Si (100) wafers were topographically modified into nano-pillars by using the photolithography and reactive ion etching (RIE) techniques. Various patterns, including nano-pillars of varying diameters and pitches (distance between pillars), were fabricated. Then, the patterns were coated with a Z-DOL (perfluoropolyether (PFPE)) lubricating film using a dip-coating technique, and this process was followed by thermal treatment. These modified surfaces were tested for their nanotribological properties, namely adhesion and friction forces, using an atomic force microscope (AFM). The results showed that the topographical modification and Z-DOL coating each independently reduced the adhesion and friction forces on the Si surfaces. However, the combination of the two surface treatments was most effective in reducing these forces. This is attributed to the combined effects of the reduction in the real area of contact due to patterning and the low surface energy of the Z-DOL lubricant. Further, it was found that adhesion and friction forces of the surfaces with combined modification varied significantly depending on the diameter of the pillars and the pitch. It is proposed that such a combination of surface modifications promises to be an effective method to improve the nanotribological performance of miniaturized devices, such as MEMS, in which Si is a typical material.

**Keywords:** Surface modification; Z-DOL; Friction; Adhesion; AFM; Micro/Nano

### 1. Introduction

Micro/Nanoelectromechanical systems (MEMS/ NEMS) and their components are traditionally made from silicon (Si) and Si-based materials [1]. A native oxide layer with hydrophilic nature (i.e., high surface energy) is always found on the Si surface, causing poor tribological properties including high adhesion and friction forces. These forces are critical for the MEMS/NEMS devices, in which the elements move relative to each other. Minimizing these forces to improve reliability and durability of the devices has become a challenge.

Water contact angle (WCA) is an indication of surface energy [2]. The higher the surface energy, the stronger the adhesion between the contacting solid surfaces becomes [2–4]. Any increase in WCA (i.e., a decrease in surface energy) will reduce adhesion. A hydrophobic surface (WCA  $\geq 90^\circ$ ) can suppress the meniscus force (a component of adhesion force in

the liquid-mediated contact) to a largely extent [4]. Consequently, the friction associated with such a surface can be decreased. In addition, the real area of contact significantly influences adhesion and friction properties [5, 6]. A reduction in the real area of contact results in a decrease in adhesion and friction. To improve the tribological properties of Si surfaces, various techniques have been used. Chemical modifications such as coatings of thin lubricating films like perfluoropolyether (PFPE) [7] or molecular organic films like self-assembled monolayer (SAM) and Langmuir-Blodgett [8, 9] are the most popular treatments. These films can lower the surface energy of treated surfaces, which, in turn, reduce adhesion and friction. Among the various films, PFPEs have been used successfully in the magnetic disk drive industry to reduce friction and wear of the disk and head [7, 10]. PFPE films, which have molecular-scale thickness, have been considered as promising candidates for MEMS/NEMS lubrication due to their hydrophobic property that supports low surface energy, good adhesion to substrates, chemical and thermal stability, and excellent lubricity [7]. On the other hand, topographical modification, that is, creating rough structures on a relatively smooth surface, has recently become of great inter-

<sup>†</sup> This paper was presented at the ICMDT 2009, Jeju, Korea, June 2009. This paper was recommended for publication in revised form by Guest Editors Sung-Lim Ko, Keiichi Watanuki.

\*Corresponding author. Tel.: +82 2 958 5651, Fax.: +82 2 958 6910

E-mail address: esyoon@kist.re.kr

© KSME & Springer 2010

est for the enhancement of their tribological properties at small scales [5, 11–14]. The topographically modified surfaces come into contact with another surface on top of the rough structures, which reduces the real area of contact, therefore reducing adhesion and friction. Under such circumstances, hydrophobic surfaces that provide a low surface energy accompanied by reduced contact area promise to be a potential solution for tribological issues at micro/nano scales.

In our previous work related to topographical modification, we fabricated polymeric nano-patterns of various aspect ratios on Si surfaces [12]. The investigation indicated that these polymeric patterns exhibited significantly lower adhesion and friction compared with the flat surface, owing to their hydrophobic nature and reduced real area of contact. More importantly, we observed that the height of the patterns strongly affected the adhesion and friction of the patterned surfaces. In our most recent work, we have focused on the combination of topographical and chemical modifications with the goal of enhancing tribological performance. The topographically and chemically modified surfaces can integrate the advantages of both modifications, that is, provide low surface energy and reduced real area of contact, thus more efficiently reducing adhesion and friction. In this study, we combined these two kinds of surface treatments for Si surfaces. The Si (100) wafers were directly patterned into nano-pillars of various diameters and pitches. The patterned surfaces were further chemically treated by coating Z-DOL (PFPE) thin films. The nanotribological properties of the combined modification surfaces were investigated and compared with those of the bare, flat Si.

## 2. Specimens and experimental details

### 2.1 Fabrication of nano-pillars

A MEMS fabrication process, which includes photolithography and RIE techniques, was used to fabricate nano-pillars on Si wafers. Fig. 1 shows the block diagram of the fabrication process of the nano-pillars. First, a thin layer of the bottom-anti-reflective coating (BARC) was spin-coated on cleaned Si wafers. Next, a photoresist (PR) thin film was then spin-coated over the BARC-deposited wafers and baked to remove the solvent. The PR film was exposed to UV light. The unexposed PR was removed with a developer solution, and the BARC layer that appeared on the surface was ashed out using inductively coupled plasma (ICP) asher. The wafers were then etched into nano-pillars by the RIE process. Finally, the remaining BARC and PR layers were removed using a plasma-ashing process, producing the required pillars. Using this process, various structures, including pillars with different diameters and pitches, were fabricated. The patterned surfaces were cleaned using piranha solution ( $\text{H}_2\text{SO}_4:\text{H}_2\text{O}_2$ , 4:1) for 10 min and were then washed using deionized (DI) water, followed by nitrogen blowing.

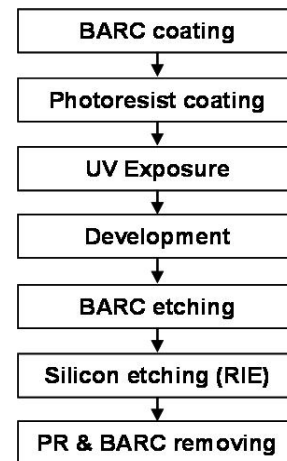


Fig. 1. Block diagram of the fabrication process (topographical modification) of Si pillars by photolithography and reactive ion etching (RIE) techniques.

### 2.2 Z-DOL coating

After fabricating the nano-pillars, the patterned surfaces were coated with a thin film of Z-DOL using the dip-coating method [7, 13]. Before coating, the samples were cleaned in acetone and isopropyl alcohol (IPA) for 5 min each, followed by DI water washing and nitrogen blowing. The cleaned samples were subsequently submerged, in the vertical direction, for 10 min in a dipping solution of Z-DOL2000 (Solvay Solexis) diluted in hydrocarbon solvent (HT70, Solvay Solexis) to 0.1% by volume. Then, the samples were vertically pulled out of the solution at a speed of 3.5 mm/s. For full bonding, after the dip-coating procedure, the samples were heated at 150°C for 30 min, and they were subsequently washed in HFE-7100 solvent (3M) for about 5 min to remove the mobile fractions. The thickness of the Z-DOL film on the flat Si substrate was measured using an ellipsometer and was determined to be approximately 2 nm.

### 2.3 Characterization of tribological properties

The morphology of the surfaces with combined modification was examined by an environmental scanning electron microscope (ESEM). Fig. 2 shows the SEM images of the topographically and chemically modified surfaces, that is, the Z-DOL-coated Si pillars. The characteristics of the fabricated surfaces, including the dimensions of the pillars, are shown in Table 1. The patterns are classified into two groups. The first group, which is comprised of S1, S2, and S3, has different pitches, while the second group, which is comprised of S1, S4, and S5, has pillars with different diameters. All the samples, including flat Si, flat Z-DOL, and Z-DOL-coated Si pillars, were examined by a contact angle analyzer (Phoenix 300, SEO) using the sessile-drop method to determine their WCA. The averaged values of WCA over five measurements are given in Table 2.

A commercial AFM (MultiMode, Nanoscope IIIa, Digital Instruments) was used to investigate the nano-adhesion and friction of the samples. Glass balls of 5  $\mu\text{m}$  in diameter mounted on Si nitride triangular cantilevers (spring constant  $\sim 0.58$  N/m, Novascan), were used as tips. The adhesion force (pull-off force) was measured in the force-displacement mode [5, 6]. The values of the force were averaged over 50 measurements in different areas of sample surfaces. Friction measurements were performed in the lateral-force-microscope (LFM) mode. The applied load was in the range of 0–80 nN. Friction force was calculated based on the trace minus retrace (TMR) values [5, 6]. The tip velocity and scan area were 5  $\mu\text{m}/\text{s}$  and 20  $\mu\text{m} \times 20 \mu\text{m}$ , respectively.

Table 1. Dimension of the fabricated nanopatterns.

Samples	Diameter (nm)	Pitch (nm)	Height (nm)	Reduced contact area (times)
S1	254	346	200	7.1
S2	254	646	200	16
S3	254	946	200	28.42
S4	554	346	200	3.36
S5	854	346	200	2.51

Table 2. WCA of the modified surfaces.

Samples	Solid/Air fractions ( $f_1/f_2$ )	Roughness factor ( $r$ )	WCA (degree)
Flat Si	-	-	35.7 $\pm$ 1
Flat Z-DOL	-	-	95 $\pm$ 3
S1	0.140/0.860	1.431	114 $\pm$ 2
S2	0.062/0.938	1.192	106 $\pm$ 2
S3	0.035/0.965	1.108	105 $\pm$ 2
S4	0.298/0.702	1.393	110 $\pm$ 2.5
S5	0.398/0.602	1.334	109 $\pm$ 3

Friction force values were averaged over 10 measurements at different areas of sample surfaces.

All experiments were conducted in a clean room with a controlled temperature of about 24 $\pm$ 1 $^\circ\text{C}$  and a relative humidity of 45 $\pm$ 5%.

### 3. Results and discussion

#### 3.1 WCA analysis

The static WCAs of flat Si, flat Z-DOL, and Z-DOL-coated Si pillars (Z-DOL/Si pillars) are given in Table 2. The flat Si shows a hydrophilic property, whereas the flat Z-DOL is hydrophobic in nature. The chemical treatment by coating Z-DOL (a low-surface-energy material) greatly increased the WCA of the flat Si surface. Interestingly, the Z-DOL/Si pillars further increased WCA, indicating that the combined modification was very effective in increasing the hydrophobicity of the flat Si surface. However, the WCA of the Z-DOL/Si pillars showed a variation in values depending on diameter of the pillars and pitch. To understand the wetting properties of the Si surfaces with the combined modification, two models of wetting, Wenzel [15] and Cassie-Baxter [16], were considered. According to the Wenzel model (homogeneous wetting), the WCA of a flat, hydrophobic surface increases with the roughness as follows:

$$\cos\theta_w = r \cos\theta_o \quad (1)$$

where  $r$  is the roughness factor (ratio of the true-solid area to its geometrical area),  $\theta_o$  is the WCA of the flat surface, and  $\theta_w$  is WCA of the Wenzel state. On the other hand, in the Cassie-Baxter model (heterogeneous wetting), a rough surface is considered as a composite consisting of solid ( $f_1$ ) and air ( $f_2$ ) fractions. The WCA increases with the air fraction as follows:

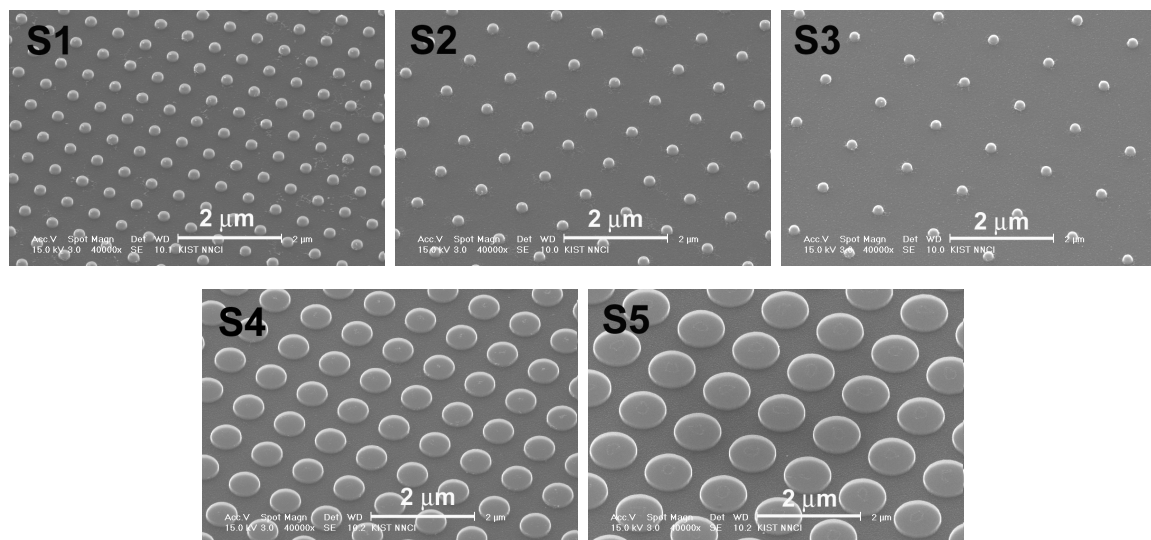


Fig. 2. SEM images of the topographically and chemically modified Si surfaces, that is, Z-DOL-coated Si pillars (Z-DOL/Si pillars). Two kinds of structure were fabricated including pillars of different diameters (S1, S4, and S5) and pillars with different pitches (S1, S2, and S3).

$$\cos\theta_c = f_1 \cos\theta_o - f_2 \quad (2)$$

where  $\theta_c$  is the WCA of the Cassie-Baxter state,  $f_1 + f_2 = 1$ .

The values of the roughness factor ( $r$ ) as well as the solid and air fractions ( $f_1$  and  $f_2$ , respectively) of the Z-DOL/Si pillars are given in Table 2. Fig. 3(a) shows the measured WCA of the Z-DOL/Si pillars as a function of the air fraction. It is observed that the WCA increases with the air fraction ( $f_2$ ) in the case of S5, S4, and S1 (the pillars with different diameters), which follows the Cassie-Baxter state. However, the WCA decreased in high air fraction in the cases of S2 and S3. This indicates that the wetting property of the nanopatterns, the cases of S2 and S3, cannot be explained by using only the Cassie-Baxter model. Fig. 3(b) shows the WCA as a function of the roughness factor ( $r$ ). The WCA of the Z-DOL/Si pillars increased with the increase in  $r$  in the cases of S3, S2, and S1. As the flat Z-DOL is hydrophobic, the experimental results indicate that the wetting property of the pillars with different pitches (S1, S2, and S3) is governed by homogeneous wetting (Wenzel state). Although the WCA of S5, S4, and S1 was observed to increase with the roughness factor, their wetting property was mainly ruled by the heterogeneous wetting, as previously mentioned. Considering Fig. 3(a), the WCA slightly increases from S5 to S4 and to S1, and then significantly decreases from S1 to S2 and to S3 with the air fraction,

suggesting that there is a transition from heterogeneous wetting to homogeneous wetting (i.e., from the Cassie-Baxter state to the Wenzel state) among the Z-DOL/Si pillars. The composite interface is unstable and can easily transform into the homogeneous interface. The transition criterion from the Cassie-Baxter state to the Wenzel state is near S1 in the present case. However, as the wetting property of the nanostructures is very complicated and is not clearly understood, further work on various structures and materials is necessary.

### 3.2 Tribological behavior

#### 3.2.1 Effect of combined surface modification

The adhesion forces of the flat Si, flat Z-DOL, representative Si pillars (S4 before coating Z-DOL), and Z-DOL/Si pillars (S4) are shown in Fig. 4(a). The flat Si exhibits the highest adhesion force due to its high surface energy [18]. The Z-DOL film greatly reduces the adhesion force of the flat Si due to its low surface energy. On the other hand, the fabrication of nano-pillars on Si wafer also greatly reduces adhesion force. The presence of the nanopillars significantly reduces the contact area of the surface (Table 1) because the AFM tips just come into contact with the surface on top of the pillars. Although the WCA of the Si pillars ( $\sim 26^\circ$ ) is lower than the flat Si wafer ( $\sim 35.7^\circ$ ), that is, the Si pillars have higher surface energy, the reduction in the contact area is the main reason for the reduction in adhesion of Si pillars. The higher surface energy of Si pillars possibly gives rise to an increase in the inherent adhesion, but the reduced area of contact is the dominant factor in determining the adhesion force in the present case. More importantly, the Z-DOL/Si pillars exhibit the lowest adhesion force compared with the rest of the surfaces tested. This is due to the combined effect of the reduced surface energy by coating with Z-DOL and the reduced area of contact by patterning. However, between the Si pillars and Z-DOL/Si pillars, the latter exhibit a much lower adhesion force despite having almost similar contact areas. Undoubtedly, this is due to the low surface energy of the Z-DOL coating. Fig. 4(b) shows the friction data of the modified surfaces compared with those of the flat Si. In Fig. 4(b), friction exhibits a similar trend to adhesion. The flat Si exhibits the highest friction force values; the flat Z-DOL and Si pillars greatly reduce friction force; and the Z-DOL/Si pillars show the lowest friction force at any given normal load. The high friction of the flat Si is mainly due to its high surface energy [17]. The creation of nano-pillars on flat Si surface greatly reduced the real contact area of the surface. According to the fundamental law of friction given by Bowden and Tabor [18], friction force is directly proportional to the real area of contact. Therefore, the reduced friction force of the Si pillars compared with flat Si is due to the reduction of the real contact area. By coating Z-DOL on the flat Si, the friction force is also reduced significantly, as Z-DOL is a lubricant with excellent lubricity [7]. In addition, the low surface energy of the Z-DOL can reduce the contact area according to the Johnson-Kendall-Roberts (JKR) theory [3]

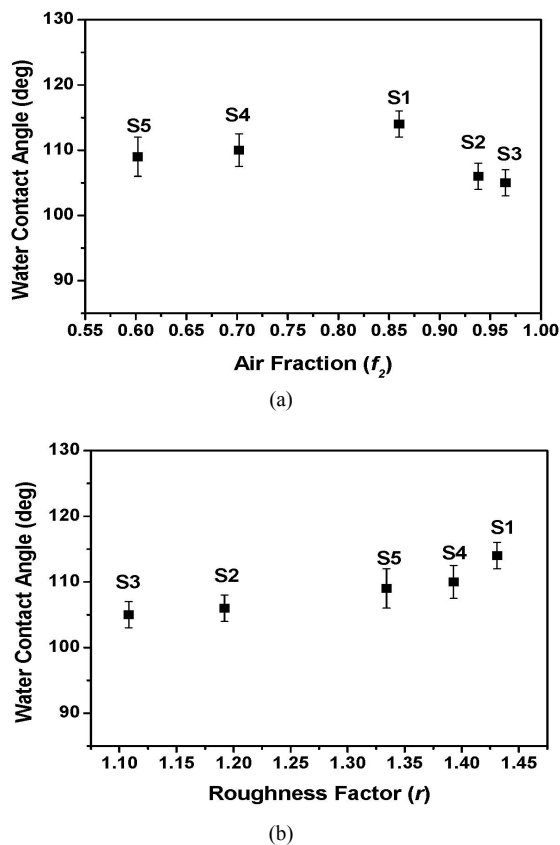


Fig. 3. WCA of Z-DOL-coated Si pillars as a function of (a) air fraction ( $f_2$ ) and (b) roughness factor ( $r$ ).

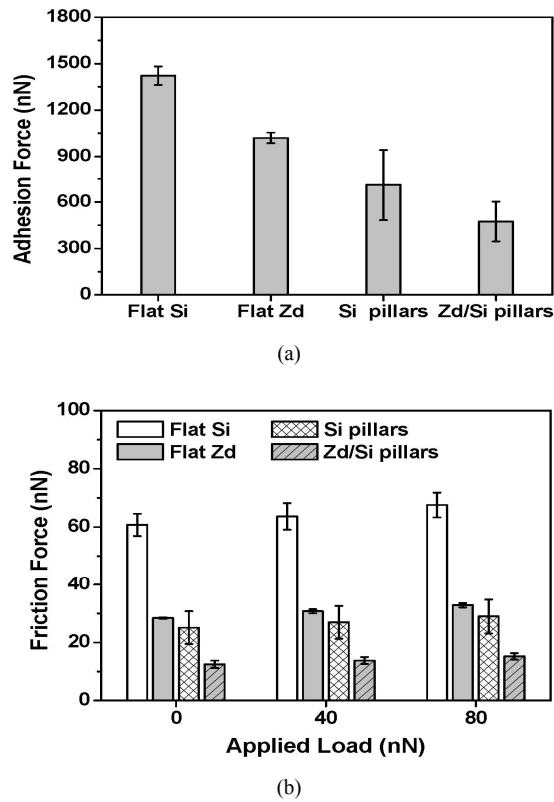


Fig. 4. (a) Adhesion force and (b) Friction force of the flat Si, Z-DOL coated on flat Si (Flat Zd), Si pillars (S4 before coating Z-DOL), and Z-DOL coated on Si pillars (Zd/Si pillars, S4).

(contact area is directly dependent on surface energy), which additionally contributes to the reduced adhesion and friction forces of the Z-DOL-coated flat Si surface. Similarly, among the Si pillars and the Z-DOL/Si pillars, the coated pillars exhibit a much lower friction force, mainly due to the excellent lubricity along with the low surface energy of the Z-DOL. Hence, these experimental results indicate that the combination of these two kinds of surface treatments can be used effectively to reduce the adhesion and friction forces of Si surfaces, owing to the combined effect of the low surface energy by coating Z-DOL and the reduced contact area by patterning.

### 3.2.2 Effect of pitch

The effects of pitch on the nanotribological properties of the modified surfaces with combined modification were examined. Specimens, namely S1, S2, and S3, which have the same pillar diameters but different pitches, were the objects for this study. Fig. 5(a) summarizes the adhesion force of the Z-DOL/Si pillars as a function of the pitch. It is seen that adhesion force decreases with the pitch values. The contact area is significantly reduced with the pitch from S1 to S2 and S3. The nominal contact area of S1 is about 2.2 times and 4 times greater than that of S2 and S3, respectively, implying that the real contact area plays a role in adhesion behavior. On the other hand, considering the WCA values, it was observed that the WCA decreased slightly with the pitch (Table 2). In view

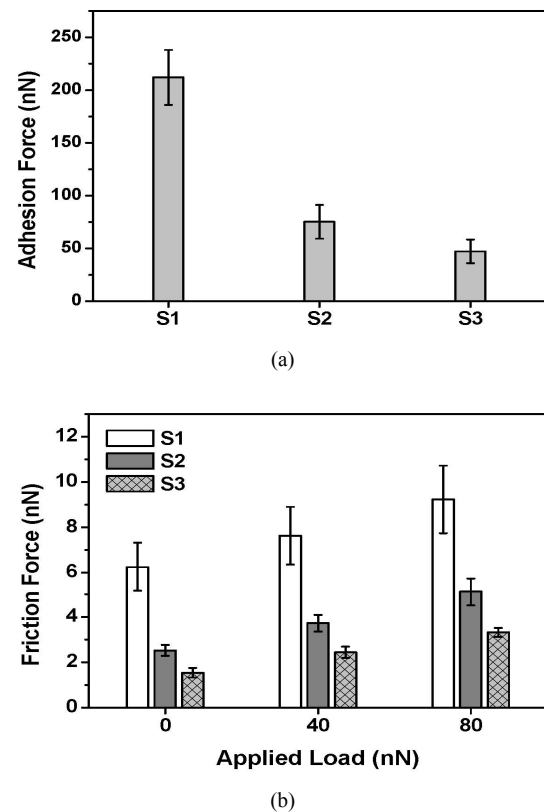


Fig. 5. (a) Adhesion force and (b) friction force of the Z-DOL/Si pillars with different pitches (S1, S2, and S3).

of surface energy, S1, which has higher WCA (i.e., lower surface energy), should have lower adhesion than S2 and S3. However, the experimental results indicate that the reduced area of contact is the main mechanism that reduces adhesion force from S1 to S2 and to S3 in the present study. Fig. 5(b) shows the friction forces of the Z-DOL/Si pillars as a function of the pitch. Similar to adhesion, friction force also decreases with pitch values at any given applied load. As the real area of contact decreases significantly from S1 to S2 and to S3 as mentioned earlier, the decrease in the real area of contact results in the reduction of friction force. Again, although there is a slight decrease in the WCA values with the pitch, the reduction in the contact area plays a major role in decreasing friction force with the pitch.

### 3.2.3 Effect of the diameter of the pillars

The effects of the pillar's diameter on adhesion and the friction behavior of the modified surfaces were examined. S1, S4, and S5, which have the same distance between the pillars but different diameters (Table 1), were selected as specimens. Fig. 6(a) shows the adhesion forces of the Z-DOL/Si pillars with different diameters. All the pillars show lower adhesion forces compared with flat Si (Fig. 4(a)), owing to their hydrophobicity and the reduced area of contact. Among these pillars, adhesion force increases with the diameter of the pillars. As shown in Table 2, the contact area (indicated by  $f_i$ ) increases with the

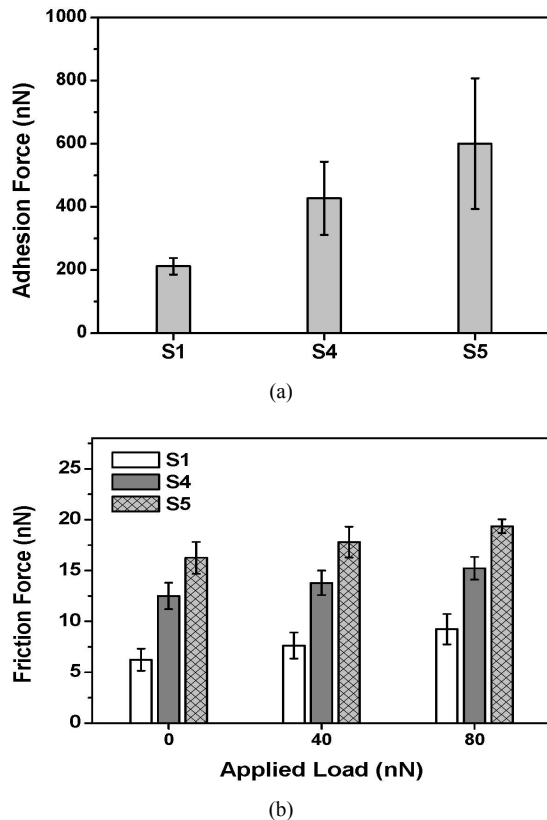


Fig. 6. (a) Adhesion force and (b) friction force of the Z-DOL/ Si pillars with different diameters (S1, S4, and S5).

diameter of the pillars. The nominal contact area of S5 is about 1.34 times and 2.83 times greater than that of S4 and S1, respectively. As the WCAs of Z-DOL/Si pillars decrease slightly with the diameter of the pillars and as the pillars are hydrophobic in nature, the reduced real area of contact is the main reason for the reduction in adhesion force with the diameter. The adhesion forces of S1, S4, and S5 were observed to be proportional to the reduction in the contact area. This experimentally demonstrates the governing role of the contact area on adhesion in the present cases. The effect of the pillar's diameter on the friction behavior of Z-DOL/Si pillars is shown in Fig. 6(b). Again, friction exhibits a trend similar to adhesion as the friction force increased with the diameter of the pillars at any given load applied. This is attributed to the increase in the real area of contact affected by the increase in the diameter of the pillars. Morphology of the modified surfaces after the tests was examined using SEM. There is no trace of damage of the surfaces, which is possibly due to such light load conditions.

#### 4. Conclusions

In this work, Si (100) wafers were modified topographically into nano-pillars and subsequently treated by coating Z-DOL films. The surfaces with combined modification were investigated for their hydrophobicity and nanotribological properties

in connection with the pillar's diameter and pitch. It was revealed that such a combined modification was very effective in increasing the hydrophobicity of the flat Si surface. A transition from heterogeneous wetting (the Cassie-Baxter state) to homogeneous wetting (the Wenzel state) was experimentally observed among the Z-DOL-coated Si pillars with increasing pitch. For the adhesion and friction properties, it was demonstrated that the adhesion and friction forces of such modified surfaces were significantly reduced due to the combined effect of the reduced area of contact by topographical modification and the low surface energy of the Z-DOL coating. Of these modified surfaces, the adhesion and friction forces increased with the pillar's diameter and decreased with the pitch. The reduced real area of contact was the main reason for such changes in these forces. We envision that the combination of topographical and chemical modifications will have potential applications for the enhancement of tribological properties of small-scale devices such as MEMS/NEMS.

#### Acknowledgment

This research was supported by the Korea Institute of Science and Technology (KIST) Institutional Program. The grant (No. 2008-E032) funded by the Ministry of Knowledge Economy.

#### References

- [1] B. Bhushan ed., Tribology issues and opportunities in MEMS, Kluwer academic, Dordrecht, The Netherlands, (1998).
- [2] B. D. Beake and G. J. Leggett, Variation of frictional forces in air with the compositions of heterogeneous organic surfaces, *Langmuir* 16 (2000) 735-739.
- [3] K. L. Johnson, K. Kendall and A. D. Roberts, Surface energy and contact of elastic solid, *Proc. R. Soc. Lond. A* 324 (1558) (1971) 301-313.
- [4] B. Bhushan, Adhesion and stiction: Mechanisms, measurement techniques, and methods for reduction, *J. Vac. Sci. Technol. B* 21 (2003) 2262-2296.
- [5] Y. Ando and I. Ino, The effect of asperity array geometry on friction and pull-off force, *Journal of Tribology* 119 (1997) 781-787.
- [6] B. Bhushan, Handbook of micro/nano tribology, CRC Press, Boca Raton, USA, (1999).
- [7] Z. Tao and B. Bhushan, Degradation mechanisms and environmental effects on perfluoropolyether, self-assembled monolayers, and diamond-like carbon films, *Langmuir* 21 (2005) 2391-2399.
- [8] R. Maboudian and R. T. Howe, Critical Review: Adhesion in surface micromechanical structures, *J. Vac. Sci. Technol. B* 15 (1997) 1-20.
- [9] A. Ulman, An introduction to ultrathin organic films from langmuir-blodgett to self-assembly, Academic Press, San Diego, USA, (1991).
- [10] B. Bhushan, Tribology and mechanics of magnetic storage

devices, Springer Verlag, New York, 1996.

- [11] Z. Burton and B. Bhushan, Hydrophobicity, adhesion, and friction properties of nanopatterned polymers and scale dependence for micro-nanoelectromechanical systems, *Nano Letters* 5 (2005) 1607-1613.
- [12] E.-S. Yoon, R. A. Singh, H. Kong, B. Kim, D.-H. Kim, H. E. Jeong and K. Y. Suh, Tribological properties of biomimetic nano-patterned polymeric surfaces on silicon wafer, *Tribology Letters* 21 (2006) 31-37.
- [13] R. A. Singh, D. C. Pham, J. Kim, S. Yang and E.-S. Yoon, Bio-inspired dual surface modification to improve tribological properties at small-scale, *Applied Surface Science* 255 (2009) 4821-4828.
- [14] R. A. Singh, E.-S. Yoon, H. J. Kim, J. Kim, H. E. Jeong and K. Y. Suh, Replication of surfaces of natural leaves for enhanced micro-scale tribological property, *Materials Science and Engineering C* 27 (2007) 875-979.
- [15] R. N. Wenzel, Resistance of solid surfaces to wetting by water, *Industrial Engineering Chemistry* 28 (1936) 988-994.
- [16] A. B. D. Cassie and S. Baxter, Wettability of porous surfaces, *Trans. Faraday Soc.* 40 (1944) 546-551.
- [17] E.-S. Yoon, R. A. Singh, H. J. Oh and H. Kong, Effect of contact area on nano/micro-scale friction, *Wear* 259 (2005) 1424-1431.
- [18] F. P. Bowden and D. Tabor, *Friction and Lubrication of Solids*, Clarendon Press, Oxford, UK (1950).



**Eui-Sung Yoon** is the Head of the Nano-bio Research Center, Nano-Science Division, Korea Institute of Science and Technology (KIST), Seoul, Korea. He received his B.S., M.S., and Ph.D. degrees in Precision Mechanical Engineering from Hanyang University, Seoul, Korea. He worked with Prof.

Bharat Bhushan at the Ohio State University on his sabbatical leave. His research interests focus on micro/nano tribology for MEMS application, biomimetic surface engineering, nanomechatronics, bio-robot, and brain signal recording system.



**Duc Cuong Pham** received his B.S and M.S. degrees in Mechanical Engineering from Hanoi University of Technology (HUT), Vietnam. He joined the International R&D Academy, Korea Institute of Science and Technology (KIST) in 2001, and received his Ph.D. degree from the University of Science and Technology,

Korea, in 2007. Dr. Pham is currently a Visiting Scientist at the NanoBio Research Center, KIST. He is also a member of the Department of Mechanical Engineering, HUT since 1993. His research interests include tribology, nanomechatronics, and surface modifications for MEMS applications.